THE FLOW OF CLASSICAL MECHANICAL CUBIC POTENTIAL SYSTEMS

M. Falconi

Department of Mathematics
Facultad de Ciencias, UNAM, C. Universitaria, México, D.F., 04510, MEX

E. A. Lacomba

Department of Mathematics, UAM-I
P.O.Box 55-534, México, D.F. 09340, MEX

C. Vidal

Department of Mathematics, Universidade Federal de Pernambuco
Cidade Universitaria, Recife-Pe, Brasil

Abstract. This paper describes the global flow of homogeneous polynomial potentials of degree 3 for negative and positive energy. For the negative energy case a blow up of McGehee type is enough to get the complete picture of the flow. In the positive energy case, McGehee blow up fails to give global information about the flow, but comparing with a separable case we are able to obtain all the possible asymptotic behavior of solutions, whenever the coefficients of the normal form of the potential are positive.

1. **Introduction.** In [4] we studied some general properties of the flow for mechanical systems with polynomial potentials of degree at most 4. The essential tool was the application of a McGehee type blow up at infinity studied systematically by Lacomba and Ibort [6]. It was generalized later in [7], where the mass matrix was assumed to depend on the position in a homogeneous way. This blow up produces a two dimensional manifold called the *infinity manifold* which allows us to study the flow in a neighborhood of the infinity in the configuration space. This method has also been applied to the study of mechanical systems with quasihomogeneous potentials, where the homogeneity degree is negative, (see [2]). In a more recent paper [5], we focused in the study of the global flow for the case of homogeneous polynomial potentials of degree 3 and negative energy. The blow up allowed us to extend the energy level to a compact three dimensional manifold with the infinity manifold as boundary. This boundary is invariant under the extended flow. Transversality properties of the flow in [5] were used to get the global flow in the case of separable potential. In this paper, we show how to extend the analysis of the separable case to the general one, when the energy is negative. Moreover, we also describe the flow for positive energy, where the blow up does not give global information, and we have to use some comparison based on differential inequalities. In Section 2 we review the McGehee blow up at infinity giving the expression of the vector field on the energy levels and the infinity surface for mechanical systems with 2 degrees of

freedom and any positive degree of homogeneity in McGehee coordinates. It turns out that the flow on the infinity surface is always gradient-like with respect to one of the velocity coordinates (see [4]). We then restate the main properties of the global flow for separable cubic homogeneous potentials when energy is negative, which were proved in [5] and turned out to be fundamental for studying the global flow in the general case.

In Section 3 we extend the previous result obtained in [5] for the global flow on negative energy levels, to the non separable homogeneous potentials. We prove that the general case for negative energy shows the same type of flow as the separable case. The topology of positive energy levels is described in Section 4. The flow for positive energy is analyzed in Section 5. The end result is that all solutions come asymptotically from infinity and go away to infinity in the configuration space for negative energy, while for positive energy we need a restriction on the coefficients. This is in strong contrast with the behavior of systems with non homogeneous polynomial potentials, where it has been shown that the dynamics is very rich, with the appearance of many periodic and recurrent orbits. This is the case for example of the classical Henon-Heiles potential where a quadratic form is added to the cubic terms, (see [8] and [9]).

2. **Some previous results and the global flow for negative energy.** We consider two degrees of freedom Hamiltonian systems of the following form

$$H\left(x, y, p_1, p_2\right) = \frac{1}{2}\left(p_1^2 + p_2^2\right) - V\left(x, y\right) \tag{2.1}$$

where V is a homogeneous function of degree 3 in the plane, i.e. $V\left(\lambda x, \lambda y\right) = \lambda^3 V\left(x, y\right)$ for any $\lambda > 0$.

For blowing up at infinity, configuration coordinates are changed into polar coordinates, but with the radial coordinate replaced by its reciprocal. The new position coordinates are ρ, θ, where

$$\rho = \frac{1}{\sqrt{x^2 + y^2}}; \ x = \frac{1}{\rho}\cos\theta; \ y = \frac{1}{\rho}\sin\theta. \tag{2.2}$$

The new radial and tangential velocity components are respectively defined as

$$v = \rho^{3/2}\left(-\dot{\rho}/\rho^2\right), \ u = \rho^{3/2}\left(\rho^{-1}\dot{\theta}\right). \tag{2.3}$$

Then the energy relation $H = h$ in ρ, θ, v, u coordinates becomes

$$\frac{1}{2}\left(u^2 + v^2\right) = U\left(\theta\right) + \rho^3 h, \tag{2.4}$$

where $U\left(\theta\right) = V\left(\cos\theta, \sin\theta\right).$

Writing Hamilton′s equations for Hamiltonian (2.1) in terms of the new variables, shows the further need for a change of time scale

$$\frac{dt}{d\tau} = \rho^{1/2}, \tag{2.5}$$

in order to eliminate this factor from the right hand side of all the equations. We obtain the following system of differential equations

$$\begin{array}{ll} \rho' = -\rho\,v, & v' = u^2 - \frac{3}{2}\,v^2 + 3\,U\left(\theta\right), \\ \theta' = u, & u' = -\frac{5}{2}u\,v + U'\left(\theta\right), \end{array} \tag{2.6}$$

where $' = d/d\tau$.

The energy level $H = h$ in the new coordinates is defined as the 3-dimensional manifold

$$E_h = \left\{ (\rho, \theta, v, u) \mid \rho > 0, \ \frac{1}{2} \left(u^2 + v^2 \right) = U(\theta) + \rho^3 h \right\}.$$

But since the energy relation (2.4) and the system of equations (2.6) are well defined at infinity, i.e. $\rho = 0$, we can glue to E_h a 2-dimensional boundary, the <u>infinity surface</u>

$$N_\infty = \left\{ (\rho, \theta, v, u) \mid \rho = 0, \ \frac{1}{2} \left(u^2 + v^2 \right) = U(\theta) \right\},$$

which is independent of h and invariant under the flow, because from (2.6) $\rho = 0$ implies $\rho' = 0$. Although E_h and N_∞ are contained in a 4-dimensional space, they can be represented in the 3-space of coordinates θ, v, u when $h < 0$ or $h > 0$. The boundary N_∞ is a surface of revolution defined only at points where $U \geq 0$.

All the equilibrium points on N_∞ are generically hyperbolic for the flow. They are located in the intersection with the plane $u = 0$ and correspond to critical points of U.

The critical points of U generate the so-called <u>homothetic</u> <u>solutions</u>. They are defined by taking $\theta \equiv \theta_0$ where $U'(\theta_0) = 0$, $u = 0$. Homothetic solutions are depicted as vertical lines for $h \neq 0$ in θ, v, u coordinates. When $U''(\theta_0) > 0$, the corresponding points of equilibrium S_+ and S_- on N_∞ are saddles. In this case the homothetic solution belongs to the transversal intersection of two dimensional stable and unstable manifolds $W^s(S_+)$ and $W^u(S_-)$ (see [5]).

The following proposition and theorem were proved in [4].

Proposition 2.1. *The flow of (2.6) is gradient-like with respect to v, as follows*
a) If $h < 0$ on $E_h \cup N_\infty$ $(\rho \geq 0)$
b) If $h \geq 0$ on N_∞ $(\rho = 0)$

Theorem 2.2. *Let $U(x, y)$ be a cubic homogeneous polynomial potential. Suppose that $h < 0$, $U(\theta_0) > 0$, $U'(\theta_0) = 0$ and $U''(\theta_0) > 0$. Then the stable manifold $W^s(S_+)$ and the unstable manifold $W^u(S_-)$ intersect transversally along the homothetic trajectory $\{\theta = \theta_0, u = 0\}$.*

The general form of a homogeneous polynomial potential of degree 3 with 2 degrees of freedom is

$$V(x, y) = ay^3 + bxy^2 + cx^2 y + dx^3.$$

We consider the normal form

$$V(x, y) = y^3 + \alpha xy^2 + \beta x^3,$$

See details in [3]. The corresponding trigonometric polynomial $U(\theta)$ of degree 3 and its derivative are given by

$$U(\theta) = V(\cos\theta, \sin\theta) = \sin^3\theta + \alpha\cos\theta\sin^2\theta + \beta\cos^3\theta, \qquad (2.7)$$

$$U'(\theta) = \sin\theta[-\alpha\sin^2\theta + (2\alpha - 3\beta)\cos^2\theta + 3\sin\theta\cos\theta].$$

It is clear that the general shape and smoothness of the infinity surface N_∞ depend upon the roots of $U(\theta)$ and of $U'(\theta)$. Generically, we have three different geometrical shapes obtained as revolution surfaces from curves having one maximum ("ovoidal shaped"), two maxima and one minimum ("peanut shaped") and one curve with three components with a maximum each ("three ovoids").

When N_∞ is peanut shaped, we denote by A_+, B_+ the attractor points on N_∞ corresponding to the maxima of U, and by $S_\pm$ the saddle points. The θ–coordinates of A_+, $S_\pm$ and B_+ are progressive; θ_* denotes the θ–coordinate of $S_\pm$. The positive part of the corresponding function $U(\theta)$ modulo 2π is defined on an interval $(I_0(\alpha,\beta), I_1(\alpha,\beta))$, of length π, with $I_0(\alpha,\beta) \in [-\pi/2, 0]$ and $I_1(\alpha,\beta) \in [\pi/2, \pi]$.

To study the behavior of the flow on N_∞, because of the symmetry

$$(\rho, \theta, v, u, \tau) \rightarrow (\rho, \theta, -v, -u, -\tau), \tag{2.8}$$

of the solutions of system (2.6), it is enough to study the behavior of the two solutions having as initial conditions the points with $\theta = I_0(\alpha,\beta)$ and $\theta = I_1(\alpha,\beta)$. Let us denote these solutions by $\gamma(\alpha,\beta)$ and $\delta(\alpha,\beta)$, respectively. These solutions allow us to find the separatrices of the flow on N_∞, and hence they determine it completely. Due to the above symmetry, it is enough to study the part where $v \geq 0$. The following result refines Theorem 7 in [5], because of assertions (6) and (7). Although the proof is essentially the same as in that paper, we rewrite it below in order to correct some misprints.

Theorem 2.3. *Let U be given by (2.7). Then, for $\alpha = 0$, there are values $0 < \beta_1 \leq \beta_2 < \beta_2^{-1} \leq \beta_1^{-1}$ of β, such that*
(1) For each $\beta \in (0, \beta_1)$, the $\omega-$limit of $\gamma(0, \beta)$ is B_+
(2) If $\beta > \beta_2$, then the $\omega-$limit of $\gamma(0, \beta)$ is A_+,
Similarly,
(3) If $\beta \in \left(0, \beta_2^{-1}\right)$, then the $\omega-$limit of $\delta(0, \beta)$ is B_+
(4) If $\beta > \beta_1^{-1}$, then the $\omega-$limit of $\delta(0, \beta)$ is A_+
(5) For $\beta = \beta_1$, the solution $\gamma(0, \beta)$ connects the two saddle points S_- and S_+. In the same way, for $\beta = \beta_1^{-1}$, the solution $\delta(0, \beta)$ connects the same saddle points on the other side of N_∞.

Moreover, For $0 < \beta < \beta_1$ there exist two intervals $J_1(\beta)$, $J_2(\beta)$ around 0, such that
(6) If $\alpha \in J_1(\beta)$, the $\omega-$limit of $\gamma(\alpha, \beta)$ is B_+
(7) If $\alpha \in J_2(\beta)$, the $\omega-$limit of $\delta(\alpha, \beta)$ is B_+

Proof. Eliminating the time in equations of motion (2.6) with $\rho = 0$ and using the energy relation (2.4), we get the equation

$$\frac{dv}{d\theta} = \frac{5}{2}\sqrt{2U(\theta) - v^2}. \tag{2.9}$$

We compare the solutions $v(\theta)$ of this equation with the solutions of a similar equation where $2U(\theta)$ is replaced by a constant $2K$, i.e.

$$\frac{dv}{d\theta} = \frac{5}{2}\sqrt{2K - v^2}. \tag{2.10}$$

By direct integration, and assuming the initial condition $v(\theta_0) = 0$, we obtain the solution

$$\bar{v}(\theta) = \sqrt{2K}\sin\frac{5}{2}(\theta - \theta_0), \tag{2.11}$$

provided that $\frac{5}{2}(\theta - \theta_0) \leq \pi/2$, i.e. $\theta - \theta_0 \leq \pi/5$.

We begin by proving 1). Let us take $\theta_0 = I_0$ and $K = \beta$ and consider the solution (2.11). In the interval $[I_0, \theta_*]$ the inequality $0 \leq 2U(\theta) - v^2 \leq 2\beta - v^2$ is

satisfied; hence in particular

$$v\left(\theta_*\right) \le \bar{v}\left(\theta_*\right) = \sqrt{2\beta}\sin\frac{5}{2}\left(\theta_* - I_0\right).$$

On the other hand $I_0 = -\arctan\beta^{1/3}$ and $\theta_* = \arctan\beta$ converge to zero as β tends to zero. Then if β is small enough, we have

$$\bar{v}\left(\theta_*\right) \le \frac{\sqrt{2\beta}}{2} < \sqrt{2U\left(\theta_*\right)}. \tag{2.12}$$

So, for this β, we have that

$$v\left(\theta_*\right) < \sqrt{2U\left(\theta_*\right)}. \tag{2.13}$$

The second inequality of (2.12) is true at least for $\beta < 1$, since $U\left(\theta_*\right) = \beta\left(1+\beta^2\right)^{1/2}$. To prove the existence of β_1, we just take the supremum of the values of β satisfying (2.13). Then one verifies that for this value $\gamma(0,\beta)$ has a saddle-saddle connection.

We now prove 2). Assume that $U\left(\theta,\beta\right)$ has the following property: There exists an interval $[\theta_0,\theta_1] \subset [I_0,\theta_*]$ such that $\theta_1 - \theta_0 \ge \pi/5$ and $\sqrt{2U\left(\theta_0\right)} = \sqrt{2U\left(\theta_1\right)} \ge \sqrt{2U\left(\theta_*\right)}$. Because of (2.11), the solution of (2.10) with $K = U\left(\theta_0\right)$ and the initial condition $v\left(\theta_0\right) = 0$, attains the value $\sqrt{2U\left(\theta_0\right)}$ before $\theta = \theta_1$. Since the right hand side of (2.10) is greater or equal than the one of (2.9) in the interval $[\theta_0,\theta_1]$, the solution γ corresponding to $U\left(\theta,\beta\right)$ will attain a value greater than $\sqrt{2U\left(\theta_*\right)}$ in the same interval. Indeed, such an interval exists for $\beta = 1$, since $\theta_* = \frac{\pi}{4} > \frac{\pi}{5}$.

We claim that if this property is valid for some value $\beta = \beta_2$, the same is true for each $\beta > \beta_2$. Indeed, $\theta_* = \arctan\beta$ is an increasing function of β. Let $\bar{\theta}\left(\beta\right)$ be the unique negative solution of the equation

$$U\left(\bar{\theta}\left(\beta\right),\beta\right) = \frac{\beta}{\left(1+\beta^2\right)^{1/2}} = U\left(\theta_*,\beta\right). \tag{2.14}$$

We will prove that $\bar{\theta}\left(\beta\right)$ is a decreasing function of β. From the implicit function theorem we get

$$3\sin\bar{\theta}\cos\bar{\theta}\left(\sin\bar{\theta} - \beta\cos\bar{\theta}\right)\frac{d\bar{\theta}}{d\beta} + \cos^3\bar{\theta} = \frac{1}{\left(1+\beta^2\right)^{3/2}}.$$

Solving for the derivative, we have

$$\frac{d\bar{\theta}}{d\beta} = \frac{\left(1+\beta^2\right)^{-3/2} - \cos^3\bar{\theta}}{3\sin\bar{\theta}\cos\bar{\theta}\left(\sin\bar{\theta} - \beta\cos\bar{\theta}\right)}.$$

¿From (2.14), we solve for $-\cos^3\bar{\theta}$, getting the equation

$$\frac{d\bar{\theta}}{d\beta} = \frac{-\beta^2\left(1+\beta^2\right)^{-3/2} + \beta^{-1}\sin^3\bar{\theta}}{3\sin\bar{\theta}\cos\bar{\theta}\left(\sin\bar{\theta} - \beta\cos\bar{\theta}\right)}.$$

Since $-\frac{\pi}{2} < \bar{\theta} < 0$, we see that $\frac{d\bar{\theta}}{d\beta} < 0$, as asserted.

Now, β_2 is the infimum of the values of β for which the ω−limit of $\gamma(0,\beta)$ is A_+. The rest of the proof from (1)-(5), follows from the symmetry $\beta \to \beta^{-1}$. Statements (6) and (7) are easily proved using a continuity argument. $\qquad\square$
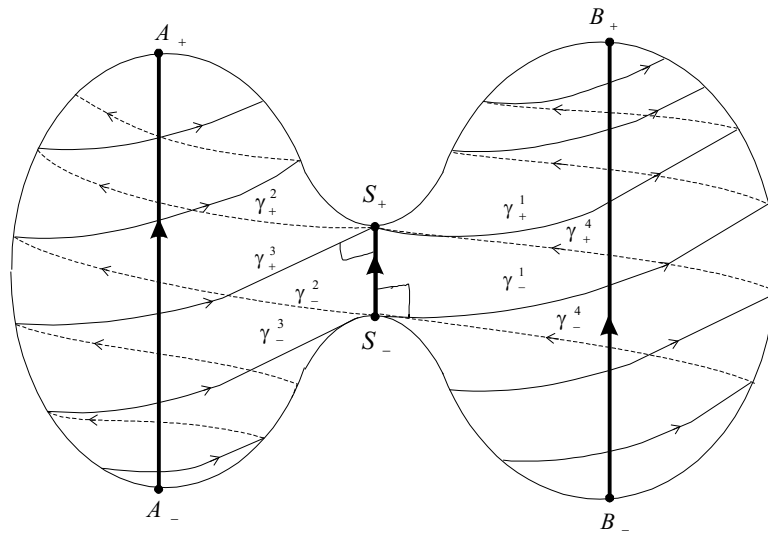
FIGURE 1

3. **Global flow for negative energy.** We will consider now the global flow on the extended energy levels $E_h \cup N_\infty$ for $h < 0$. In this case these extended levels are compact manifolds with boundary. In fact, their topology is generically one or three disjoint copies of a closed 3–ball D^3. Their flow is gradient-like everywhere, and it is completely described by the blow up coordinates. The only case where the global flow needs to be explicitly described is for the peanut shaped manifolds. For the ovoidal cases, the flow begins in a repeller and ends in an attractor for each connected component. In [5] we gave a thoroughly qualitative description for the case $\alpha = 0$, depending only on the behavior of some separatrix curves and the transversal invariant submanifolds $W^s(S_+)$ and $W^u(S_-)$. We recall the main features of this description, giving a more clear account of the construction. Generically and by symmetry, it is enough to consider two cases: $\beta_2 < \beta < \beta_2^{-1}$ and $\beta < \beta_1$. We denote by $\gamma_i^{\pm}$ the separatrix curves which are the invariant manifolds at the saddle equilibrium points on N_∞. Here, the plus sign denotes unstable manifold while the minus sign denotes stable manifolds, for $i = 1, 2, 3, 4$, (see Figure 1).

Since the flow is almost–gradient, the ω−limit of γ_1^+ and γ_2^+ are B_+ and A_+, respectively, while the ω−limit of γ_3^- and γ_4^- are A_- and B_-, respectively.

It is important to notice that the asymptotic behavior of solutions γ and δ determine the behavior of the other $\gamma_i^{\pm}$. 1) Case $\beta_2 < \beta < \beta_2^{-1}$. This is the simplest one. From Theorem 2.3 and the symmetry 2.8 the α−limit of γ is A_- and the α−limit of δ is B_-. From the same symmetry the coordinate θ of γ is always lesser than θ^* and greater than θ^* for δ. This forces the following behavior of γ_1^-, γ_2^-, γ_3^+, γ_4^+. The invariant submanifolds $W^s(S_+)$ and $W^u(S_-)$ will match with separatrices $\gamma_\pm^i, i = 1, 2, 3, 4$, at the opposite point, as shown in Figure 1.

Hence, this intersection acts as a double hinge (see Figure 2), which separates completely the flow into 4 disjoint regions in E_h. In this way, an orbit which begins at A_- may end at either A_+ or B_+. The same thing for orbits beginning at B_-.

2) Case $\beta < \beta_1$. As in the previous case, separatrices on the right have B_+ as ω−limit and B_- as α−limit. However, the unstable separatrix γ_-^2 having S_-
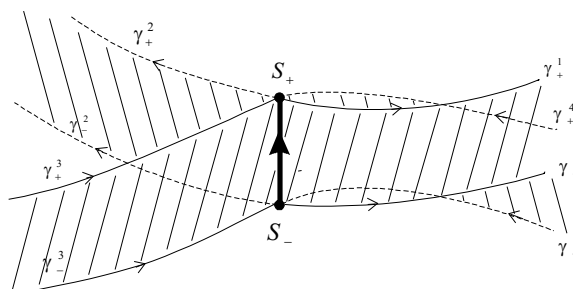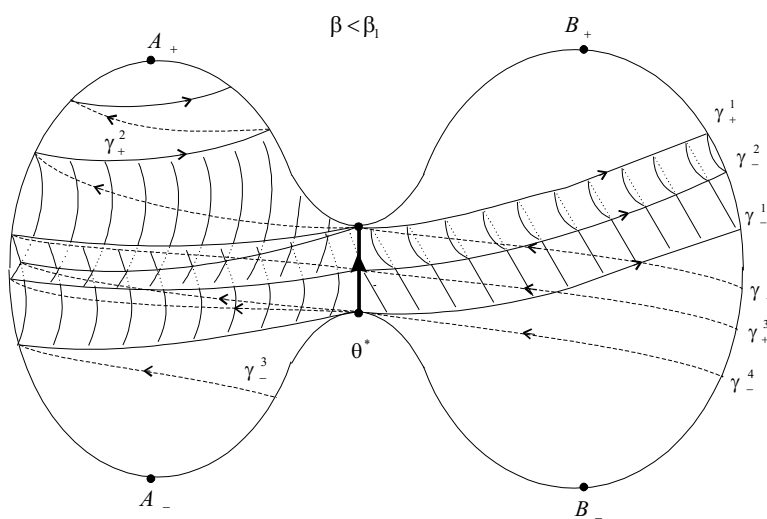
FIGURE 2

FIGURE 3

as $\alpha-$limit has B_+ as $\omega-$limit instead of A_+, while separatrix γ_-^3 having S_+ as $\omega-$limit goes around and has B_- as $\alpha-$limit instead of A_-. Hence, the double hinge described in the first case, separates the energy level into five regions in a more complicated way as we describe below.

Since γ_-^2 has B_+ as $\omega-$limit, it crosses to the right side after one turn around the homothetic orbit, while γ_+^2 stays always on the left. This forces a splitting of the corresponding invariant surface into two portions: one of them stays on the left, while the other one passes to the right. The first one is generated between two consecutive turns of γ_+^2. The other one runs between γ_+^1 and the part of γ_-^2 on the right side, but closer to N_∞ than the invariant manifold bounded by $\gamma_\pm^1$ (unstable manifold of S_-). We call this second portion a *small channel*, because of the way it runs closer to N_∞, see Figure 3.

Transversal sections $\theta < \theta^*$, $\theta = \theta^*$ (passing through S_+ and S_-) and $\theta > \theta^*$ of Figure 3 are depicted in the Figure 4. The boundary of the regions are sections of the invariant submanifolds $W_{S_-}^u$ and $W_{S_+}^s$.

In section $\theta > \theta^*$ a big new region numbered 4 appears, corresponding to the side of the double hinge containing the homothetic orbit from B_- to B_+ for $\theta > \theta^*$.
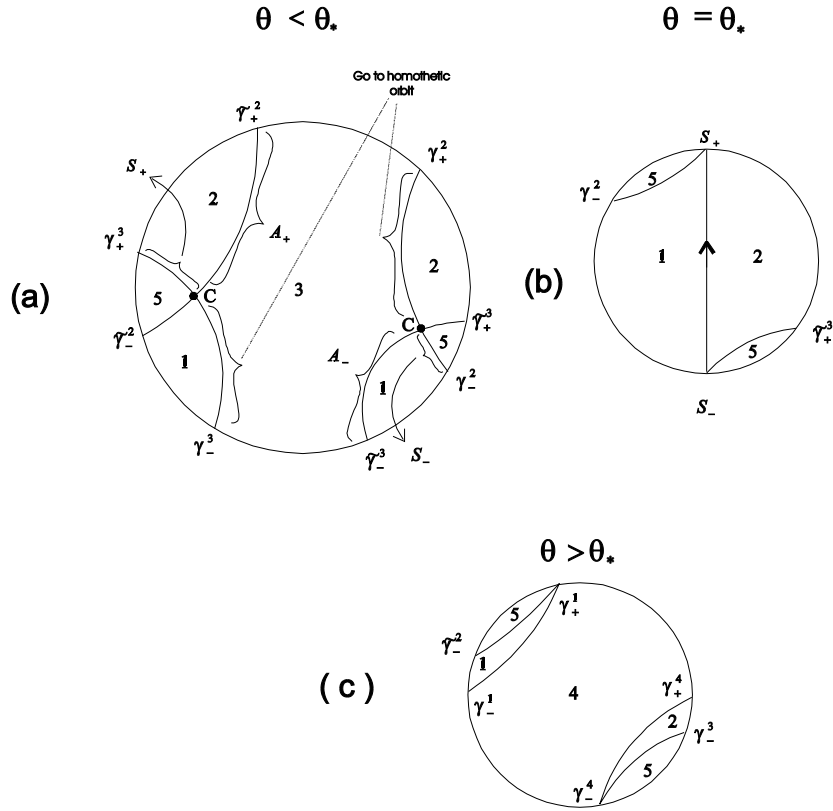
$$\theta < \theta_*$$ $$\theta = \theta_*$$

$$\theta > \theta_*$$

FIGURE 4

Regions 1, 2 and 5 have now shrunk. The last one is the continuation of the small channel.

This way we can describe precisely the $\alpha-$ and $\omega-$ limits of orbits on the 5 open regions as follows

Region	$\alpha - \text{limit}$	$\omega - \text{limit}$
1	A_-	B_+
2	B_-	A_+
3	A_-	A_+
4	B_-	B_+
5	B_-	B_+

.

Finally, the only portions of invariant submanifolds changing from one side to the other of Figure 4 for the extended energy level are

- a: The boundary between regions 1 and 5, contained in $W_{S_-}^u$. Its $\omega-$limit is B_+, exactly like γ_-^2
- b: The boundary between regions 2 and 5, contained in $W_{S_+}^s$. Its $\alpha-$limit is B_-, exactly like γ_+^3.

Basically, the two above described flows are the only ones for the general "peanut shaped" case with $\alpha \neq 0$. In fact, for $0 < \beta < \beta_1$, we recall from Theorem 2.3 there exist intervals $J_1(\beta)$ and $J_2(\beta)$ such that if $\alpha \in J_1(\beta)$, the $\omega-$limit of γ is B_+, and
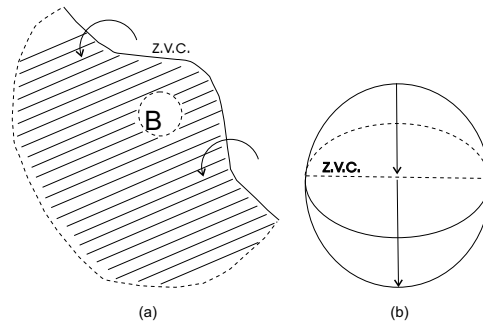
FIGURE 5

if $\alpha \in J_2(\beta)$, the $\omega-$limit of δ is B_+. By taking $\alpha \in J_1(\beta) \bigcap J_2(\beta)$, we have small channels as in case 2.

It is interesting to notice that all the trajectories are *parabolic*, which means that they escape to infinity with asymptotic velocity equal to 0. This follows from the fact that in McGehee coordinates, solutions escape towards equilibrium points on the infinity manifolds which have coordinates $\rho = 0$, $u = 0$ and $v \neq 0$. Hence, since $v = -\rho^{-1/2}\dot{\rho}$, we see that $\dot{\rho}$ tends to 0 along escaping solutions.

4. **Topology of $E_h \bigcup N_\infty$ for $h > 0$.** To describe the topology of the phase space for energy $h > 0$, we have to consider two cases: (1) when N_∞ is topologically a sphere S^2, and (2) when N_∞ has three connected components, each one topologically equivalent to a sphere S^2. We claim that in case (1) we get a closed 3–ball D^3, while in case (2) we have a D^3 where two disjoint open balls has been removed. The result in case (1) is remarkably the same as for $h < 0$.

As a verification, we will give two arguments to obtain the topology. First, by using cartesian coordinates, and second starting with blow up coordinates. In case (1), from the energy relation $\frac{1}{2}\left(p_1^2 + p_2^2\right) - V(x, y) = h$, where V is a homogeneous polynomial of degree 3 in the plane, one realizes that we have to construct an S^1 pinched bundle over the Hill's region in cartesian coordinates as it is shown in Figure 5(a). The pinching of the circles occurs on the boundary of the zero velocity curve. The dotted part of the boundary represent escape to infinity, so that it will generate N_∞. This gives a close 3–ball D^3 whose boundary is the sphere N_∞. See Figure 5(b), where the homothetic orbit is shown and the zero velocity curve appears as a dotted line intersecting it. If we start the description in blow up coordinates, we have an open solid torus obtained by identifying both ends of the cylinder in Figure 6(a). Since these coordinates can not describe a passing through the origin in configuration space, the homothetic orbit has to be completed by the homothetic dotted curve outside the cylinder. The solid torus represents in fact, the portion of E_h obtained when a small open ball B centered at the origin in Figure 5(a) is removed. As a trivial bundle over S^1, the 2–ball B generates another solid torus as it is shown in Figure 6(c), under top and bottom identification. The boundary $S^1 \times S^1$ of the solid torus has to be identified with the boundary of the solid torus in Figure 6(a), which is reproduced schematically in Figure 6(b). In this case, meridians and parallels of the two $S^1 \times S^1$ tori are exchanged when making the identification. This is known to produce topologically a 3–sphere S^3. But, since
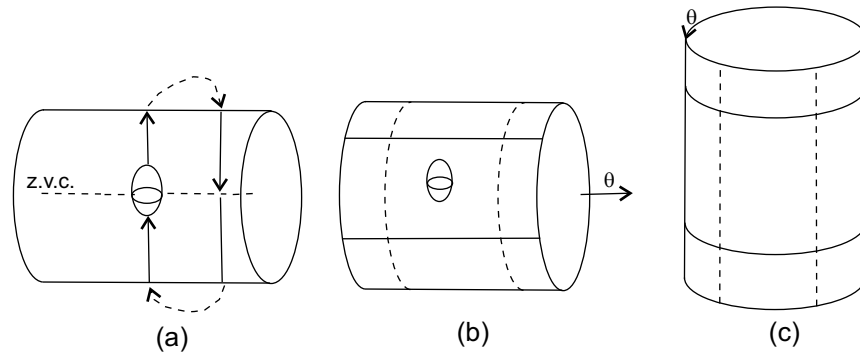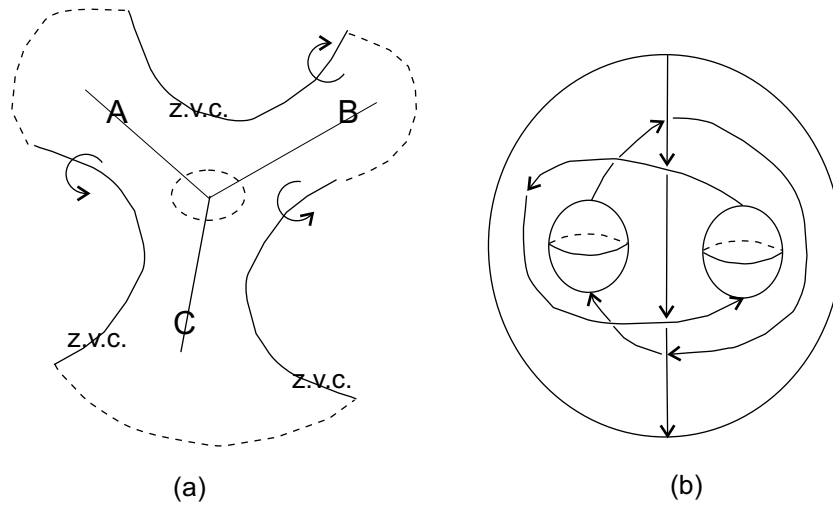
FIGURE 6

FIGURE 7

the open ball inside Figure 6(b) has to be removed, we get an S^3 where an open ball is deleted, which in turn is equivalent to a closed 3–ball D^3.

In case (2), in cartesian coordinates, we have to construct an S^1–pinched bundle over the Hill's region shown in 7(a). The pinching of the circles occurs over the boundary consisting of three disjoint zero velocity curves. In order to find the topology, we first cut Hill's region through the line segment A, B, C from the origin. Proceeding as in case (1), we get three double truncated cones as shown in Figure 8(a), (b) and (d), where conical boundaries A', B', C' have to be identified in the indicated senses.

If we identify boundaries B' in Figure 8(a) and (b), we get Figure 8(c) which is a similar solid where an open ball has been removed in its interior. Finally, boundaries A' in Figures 8(c) and (d) are correspondingly identified, giving the 3–ball D^3 where three open smaller open balls are removed in its interior, as shown in Figure 8(e). The surfaces A', B', and C' are also depicted there for an easy understanding of the process. If we start the description in blow up coordinates, the construction is similar to case (1). We have again two solid tori obtained from
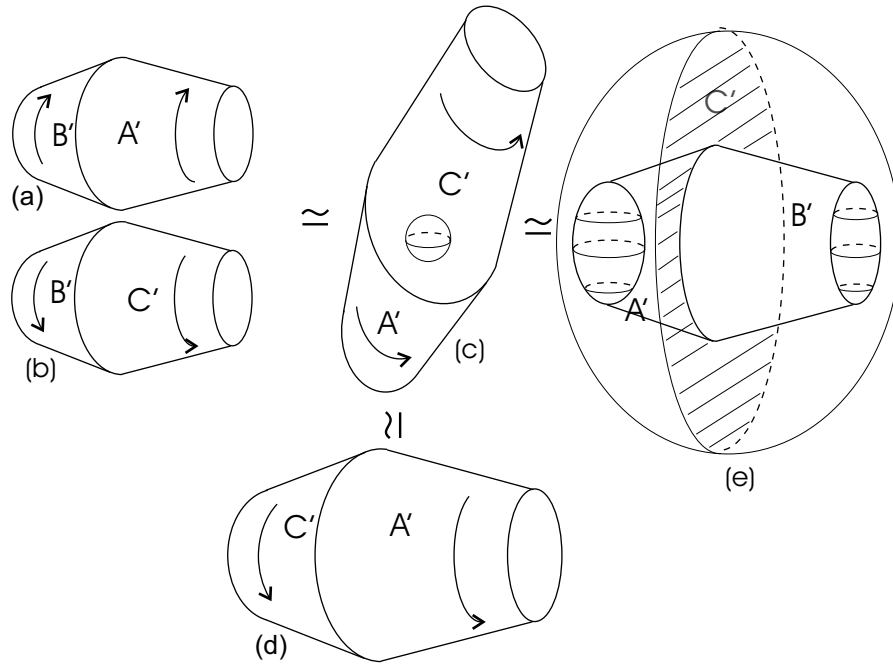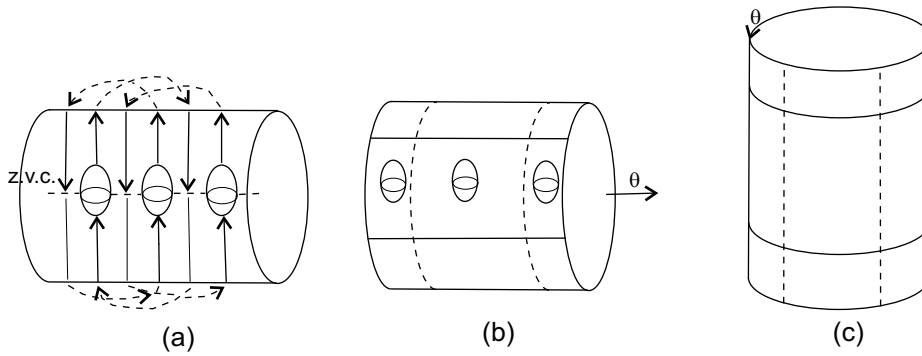
FIGURE 8

FIGURE 9

Figure 9(b) and (c) with the corresponding identification exchanging meridians with parallels.

The only difference being that we have now removed three interior small disjoint open balls in the first solid torus. The solid torus in Figure 9(c) comes from the small open ball about the origin in configuration space shown in Figure 7(a). In short, we get a 3–sphere S^3 where three disjoint small open balls are removed in its interior, which is in turn equivalent to a D^3 where two small disjoint open balls are removed in its interior, as before.

5. **Global flow for positive energy.** To study the global flow of the Hamiltonian system

$$\dot{x} = p_1, \qquad \dot{y} = p_2, \tag{5.1}$$
$$\dot{p}_1 = \alpha y^2 + 3\beta x^2, \quad \dot{p}_2 = 3y^2 + 2\alpha xy. \tag{5.2}$$

we consider first the case $\alpha = 0$

$$\dot{x} = p_1, \qquad \dot{y} = p_2, \\ \dot{p}_1 = 3\beta x^2, \quad \dot{p}_2 = 3y^2. \tag{5.3}$$

Then, the separable homogeneous potential U is given by $U(x,y) = y^3 + \beta x^3$ and the Hamiltonian is

$$H = \frac{1}{2} \left(\dot{p}_1^2 + \dot{p}_2^2 \right) - U(x,y). \tag{5.4}$$

This is an integrable system with first integrals given by

$$I_1 = \tfrac{1}{2}\dot{x}^2 - \beta x^3, \\ I_2 = \tfrac{1}{2}\dot{y}^2 - y^3. \tag{5.5}$$

The dynamics of system (5.3) on a given positive energy level $H = h$, can be reduced to the study of the dynamics of the corresponding systems in x and y on the energy levels $I_1 = h_1$ and $I_2 = h_2$ with $h = h_1 + h_2$. According to the sign of the energy levels h_1 and h_2 we have four cases: (I) $h_1 > 0$, $h_2 > 0$; (II) $h_1 < 0$, $h_2 > 0$; (III) $h_1 > 0$, $h_2 < 0$; (IV) $h_1 = 0$, or $h_2 = 0$. The Hill's region on variables x and y are respectively given by

$$x > -\left(\tfrac{h_1}{\beta} \right)^{1/3}, \\ y > -h_2^{1/3}. \tag{5.6}$$

We immediately conclude from here that for each energy level h, the coordinates of the trajectories are bounded below by the values $-\left(\tfrac{h_1}{\beta} \right)^{1/3}$ and $-h_2^{1/3}$; in particular the point $\left(-\left(\tfrac{h_1}{\beta} \right)^{1/3}, -h_2^{1/3} \right)$ is on the zero velocity curve.

Consider the initial condition $x_0 = x(0)$ and $y_0 = y(0)$ and denote by $t(x; x_0)$ the time when the solution starting at x_0 is at the position x. From the equality $I_1 = h_1$ we get

$$t(x, x_0) = \pm \int_{x_0}^{x} \frac{ds}{\sqrt{2(h_1 + \beta s^3)}}. \tag{5.7}$$

In order to compute the time of escape to infinity we choose the positive sign and to compute the time it takes for coming from infinity we take the negative sign. Similarly, the corresponding time for y is denoted by $t(y, y_0)$ and it is given by

$$t(y, y_0) = \pm \int_{y_0}^{y} \frac{ds}{\sqrt{2(h_2 + s^3)}}. \tag{5.8}$$

The time of escape to infinity of the variables x and y are denoted by $t^*(\beta; x_0) = \lim_{x \to \infty} t(x, x_0)$ and $t^*(y_0) = \lim_{y \to \infty} t(y, y_0)$, respectively. We also define the passing time through minimal values of x by

$$t_*(\beta; x_0) = \lim_{x \to -\left(\frac{h_1}{\beta} \right)^{1/3}} \int_{x}^{x_0} \frac{ds}{\sqrt{2(h_1 + \beta s^3)}}. \tag{5.9}$$

In the same way, the corresponding passing time of y is

$$t_* \left(y_0\right) = \lim_{x \to -h_2^{1/3}} \int_x^{x_0} \frac{ds}{\sqrt{2\left(h_2 + s^3\right)}}. \tag{5.10}$$

Since for each variable the intervals of definition of the solution are symmetrical with respect to the passing time through a minimal value of the corresponding variable, the times of capture from infinity are given by $T\left(\beta; x_0\right) = -t^*\left(\beta; x_0\right) - 2t_*\left(\beta; x_0\right)$ and $T\left(y_0\right) = -t^*\left(y_0\right) - 2t_*\left(y_0\right),$ respectively.

Lemma 5.1. *All the trajectories of the System (5.3), come from and escape to infinity in a finite time.*

Proof. We first analyze the case (I): $h_1 > 0$, $h_2 > 0$. We consider $x_0 > -\left(\frac{h_1}{\beta}\right)^{1/3}$ and let $K \geq 0$ be any number greater than x_0, then

$$t^*\left(\beta; x_0\right) = \int_{x_0}^K \frac{ds}{\sqrt{2\left(h_1 + \beta s^3\right)}} + \int_K^\infty \frac{ds}{\sqrt{2\left(h_1 + \beta s^3\right)}}. \tag{5.11}$$

The first integral in the above equation is finite because its integrand is continuous. On the other hand, if $s > 0$ then

$$\frac{1}{\sqrt{2\left(h_1 + \beta s^3\right)}} < \frac{1}{\sqrt{2\beta s^3}}. \tag{5.12}$$

Therefore,

$$\int_K^\infty \frac{ds}{\sqrt{2\left(h_1 + \beta s^3\right)}} = \lim_{x \to \infty} \int_K^x \frac{ds}{\sqrt{2\left(h_1 + \beta s^3\right)}} \leq \lim_{x \to \infty} \int_K^x \frac{ds}{\sqrt{2\beta s^3}} < \infty. \tag{5.13}$$

It follows that $t^*\left(\beta\right)$ is finite. By taking $\beta = 1$, we see that t^* is also finite.

To prove that $t_*\left(\beta; x_0\right)$ and $t_*\left(y_0\right)$ are finite, we take the inverse of the function $y = 1/\sqrt{2\left(h_1 + \beta s^3\right)}$ in the interval $s \in \left(-\left(h_1/\beta\right)^{1/3}, 0\right]$. So, we find that $s = \left(\frac{1}{2\beta y^2} - \frac{h_1}{\beta}\right)^{1/3}$ for $y \in \left(\frac{1}{\sqrt{2h_1}}, \infty\right)$. Thus, we see that $t_*\left(\beta; x_0\right)$ is equal to

$$t_*\left(\beta; x_0\right) = -\left(\frac{h_1}{\beta}\right)^{1/3} \left(\frac{1}{\sqrt{2h_1}}\right) - \int_{1/\sqrt{2h_1}}^\infty \left[\left(\frac{h_1}{\beta}\right)^{1/3} + \left(\frac{1}{2\beta y^2} - \frac{h_1}{\beta}\right)^{1/3}\right] dy. \tag{5.14}$$

By using the identity $\left(a^3 + b^3\right) = \left(a + b\right)\left(a^2 - ab + b^2\right),$ and after some simplifications, the above integrand becomes

$$\frac{1}{2\beta y^2 \left(\left(h_1/\beta\right)^{2/3} + \left(-h_1/\beta\right)^{1/3}\left(1/2\beta y^2 - h_1/\beta\right)^{1/3} + \left(1/2\beta y^2 - h_1/\beta\right)^{2/3}\right)}. \tag{5.15}$$

It is lesser or equal than $1/\left(2\beta\left(h_1/\beta\right)^{2/3} y^2\right)$, because the three terms in the denominator are positive. Then

$$0 \leq \int\limits_{1/\sqrt{2h_1}}^{\infty} \left[\left(\frac{h_1}{\beta} \right)^{1/3} + \left(\frac{1}{2\beta y^2} - \frac{h_1}{\beta} \right)^{1/3} \right] dy \leq$$

$$\int\limits_{1/\sqrt{2h_1}}^{\infty} 1/(2\beta \, (h_1/\beta)^{2/3} \, y^2) \, dy. \quad (5.16)$$

Hence, $t_* \, (\beta; x_0)$ is finite. The time $t_* \, (y_0)$ is also finite, since it is equal to $t_* \, (1; y_0)$.

We see now the case (II) $h_1 < 0$, $h_2 > 0$. Obviously, it follows from the previous case (I) that the times $t^* \, (y_0)$ and $t_* \, (y_0)$ are finite. Let $x_0 > - \, (h_1/\beta)^{(1/3)} > 0$. We take $s_0 > x_0$ such that $-h_1 < \frac{\beta s_0^3}{2}$. Then $-\frac{\beta s^3}{2} < h_1$ for all $s \geq s_0$. Consequently, we obtain that $\frac{1}{\sqrt{2(h_1+\beta s^3)}} < \frac{1}{\sqrt{\beta s^3}}$; therefore $t^* \, (\beta; x_0) \leq \int_{x_0}^{\infty} \frac{1}{\sqrt{\beta s^3}} ds < \infty$. In a similar way, as in case (I), the expression for $t_* \, (\beta; x_0)$ is

$$\left(x_0 + (h_1/\beta)^{1/3} \right) y_0 - \int\limits_{y_0}^{\infty} \left[\left(\frac{h_1}{\beta} \right)^{1/3} + \left(\frac{1}{2\beta y^2} - \frac{h_1}{\beta} \right)^{1/3} \right] dy, \quad (5.17)$$

where $y_0 = 1/\sqrt{2 \, (h_1 + \beta x_0^3)}$. The above integral is finite since the integrand can be taken to the form given by (5.15) and it is bounded above by $1/(2\beta \, (h_1/\beta)^{2/3} \, y^2)$. Thus $t_* \, (\beta; x_0) < \infty$.

Case (III) $h_1 > 0$, $h_2 < 0$, follows from the previous case, since $t^* \, (1; y_0) = t^* \, (y_0)$ and $t_* \, (1; y_0) = t_* \, (y_0)$.

To prove case (IV): $h_1 = 0$, or $h_2 = 0$, it is enough to analyze $h_1 = 0$. Let $x_0 > 0$. We easily see that $t^* \, (\beta; x_0) = \int_{x_0}^{\infty} \frac{ds}{\sqrt{2\beta s^3}}$ is finite and $t_* \, (\beta; x_0) = \int_0^{x_0} \frac{ds}{\sqrt{2\beta s^3}}$ is infinite. However, since $h_2 > 0$, the corresponding time for y_0 is finite and therefore the trajectory passing by (x_0, y_0) either escapes to infinity or is captured from infinity in finite time. $\square$

In what follows we give a complete description of the way the trajectories come from or go towards infinity.

Case (I): $h_1 > 0$, $h_2 > 0$. the times of escape and capture are finite and the possible intervals of definition of trajectories $(x \, (t), y \, (t))$ are: (i) $T \, (y_0) < t < t^* \, (y_0)$, (ii) $T \, (y_0) < t < t^* \, (\beta; x_0)$, (iii) $T \, (\beta; x_0) < t < t^* \, (\beta; x_0)$ and (iv) $T \, (\beta; x_0) < t < t^* \, (y_0)$. If (i) holds, coordinate $x \, (t)$ remains bounded and hence the trajectory comes from and escapes to infinity in the direction of the y axis (see (A) in Figure 10). Regarding (ii), $y \, (t)$ remains bounded when $x \, (t)$ escapes to infinity and conversely $x \, (t)$ is bounded and $y \, (t)$ goes to infinity as $t \to T \, (y_0)$. Therefore, the trajectory escapes in the direction of the x axis and is captured from infinity in the direction of the y axis (see (B) in Figure 10). In case (iii) $y \, (t)$ remains bounded and then the trajectory comes from infinity and escapes to infinity in the direction of the x axis (see (C) in Figure 10). If (iv) holds, $x \, (t)$ tends to infinity when $t \to T \, (\beta; x_0)$ and $y \, (t)$ remains bounded. Moreover, when $t \to t^* \, (y_0)$, $y \, (t)$ tends to infinity and $x \, (t)$ remains bounded; from this we see that trajectory $(x \, (t), y \, (t))$ comes from infinity in the direction of the x axis and goes to infinity in the direction of the y axis (see (D) in Figure 10). In all the cases, the trajectory may cross the x axis or the y axis.
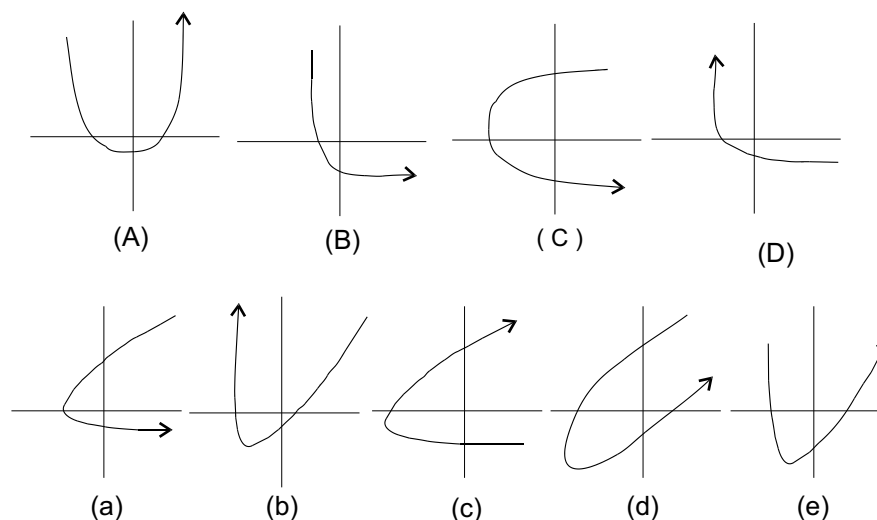
FIGURE 10

We notice that in the four cases (i)–(iv), the trajectories escape in the direction of the homothetic solution, when the times $t^*(y_0)$ and $t^*(\beta; x_0)$ are equal. Similarly, the trajectory is captured from infinity in the direction of the homothetic solution when the times $T(y_0)$ and $T(\beta; x_0)$, are equal (see (a)-(e) in Figure 10).

The cases (II): $h_1 < 0$, $h_2 > 0$ and (III): $h_1 > 0$, $h_2 < 0$, are similar to case (I), since times $T(y_0)$, $T(\beta; x_0)$, $t^*(y_0)$ and $t^*(\beta; x_0)$ are finite. Nevertheless, in case (II), the trajectory does not cross the y axis and in case (III) it does not cross the x axis.

If (IV) holds: $h_1 = 0$ or $h_2 = 0$, then $T(\beta; x_0) = -\infty$ or $T(y_0) = -\infty$, respectively. Hence, the possible intervals of definition of the trajectories when $h_1 = 0$, are: (a) $T(y_0) < t < t^*(y_0)$, (b) $T(y_0) < t < t^*(\beta; x_0)$. So, the trajectories come from infinity in the direction of the y axis and for the interval (a) they escape to infinity in the direction of the y axis, while for the interval (b) they escape in the direction of the x axis. If $t^*(y_0) = t^*(\beta; x_0)$, then the trajectory escapes with an angle $\arctan(\beta)$. The same thing happens when $h_2 = 0$, by exchanging x with y.

5.1. **The general case.** Now we consider the general case when the potential is

$$U(x, y) = y^3 + \alpha x y^2 + \beta x^3, \tag{5.18}$$

and α, β are greater than zero. System (5.3) becomes

$$\begin{aligned} \dot{x} &= p_1, & \dot{y} &= p_2, \\ \dot{p}_1 &= \alpha y^2 + 3\beta x^2, & \dot{p}_2 &= 3y^2 + 2\alpha xy. \end{aligned} \tag{5.19}$$

The analysis of the above system is reduced to that of (5.3) because of the differential inequality $\dot{p}_1 = \alpha y^2 + 3\beta x^2 > 3\beta x^2$. In order to study the behavior of variable x, we compare with the system $\dot{X} = P_1$, $\dot{P}_1 = 3\beta X^2$. We conclude from here that if variable X escapes then x escapes, and this happens in finite time. During this finite time interval y may (generically) either remain bounded or escape to infinity. This produces several cases, according to the fact that the escaping time of y be smaller, equal or greater than the the corresponding escaping time for x. It is easy

to verify that all these cases may arise, as it was the case for the integrable system (5.3), and as a consequence the escapes are as in the above described types (see Figure 10).

The idea in order to prove that coordinate $x(t)$ of each solution is bounded below goes as follows: suppose that $x(t)$ goes to $-\infty$ (on a time $T \geq -\infty$). Since $\ddot{x}$ is greater that zero, $x(t)$ is an upward concave curve, its derivative p_1 tends to a non negative value as $t \to T$. On the other hand, we see from (5.19) that $\dot{p}_1$ goes to infinity as $t \to T$. This a contradiction, because p_1 is monotonically increasing.

Although the McGehee coordinates do not give global information in the present case (positive energy), we see by using the same arguments as in the negative energy case at the end of the Section 3, that all solutions also escape parabolically to infinity.

We finally remark the importance of taking α and $\beta > 0$, in order to have the above simple dynamics. Rod [10] analyzes the Hamiltonian system corresponding to the potential $1/3x^3 - xy^2$, finding a very complicated behaviour.

REFERENCES

[1] Cushman, R.H.(1982): Geometry of the bifurcations of the normalized reduced Henon-Heiles familiy, *Proc. R. Soc. London* **A382**, 361-371

[2] Diacu, F.N.(1996): Near-collision dynamics for particle systems with quasihomogeneous potentials, *J. Differential Equations* **128**(1), 58–77

[3] Falconi, M.(1996): Estudio asintótico de escapes en sistemas Hamiltonianos Polinomiales. *Ph.D. Dissertation UNAM, Mexico*

[4] Falconi, M. and Lacomba, E.A.(1996): Asymptotic behavior of escape solutions of mechanical systems with homogeneous potentials, *Cont. Math.* **198**, 181-195

[5] Falconi, M., Lacomba, E.A. and Vidal, C.(2001): Global dynamics of mechanical systems with cubic potentials, *Qual. Th. Dynam. Sys* **2**, 429-453

[6] Lacomba, E.A. and Ibort, L.A.(1988): Origin and infinity manifolds for mechanical systems with homogeneous potentials, *Acta App. Math.* **11**, 259-284

[7] Lacomba, E.A., Bryant, J. and Ibort, L.A.(1991): Blow up of mechanical systems with a homogeneous energy, *Publ. Mat.* **35**, 333-345

[8] Llibre, J. and Simó, C.(1981): On the Henon-Heiles potential, *III Congreso de Ecuaciones Diferenciales y Aplicaciones, U. de Santiago de Compostela*, 183-206

[9] Lichtenberg, A.J. and Lieberman, M.A.(1992): *Regular and chaotic dynamics*, second edition, Applied Mathematical Sciences **38**, Springer-Verlag, New York

[10] Rod, D.L.(1973): Pathology of invariant sets in the monkey saddle, *J. Differential Equations* **14**, 129-170

E-mail address: `falconi@servidor.unam.mx, lace@xanum.uam.mx,`
E-mail address: `claudio@riemann.dmat.ufpe.br`